Vehicle System Dynamics: International Journal of Vehicle Mechanics and Mobility

Publication details, including instructions for authors and subscription information:
http://www.tandfonline.com/loi/nvsd20

Economy-oriented vehicle adaptive cruise control with coordinating multiple objectives function

Shengbo Eben Li [a], Keqiang Li [a] & Jianqiang Wang [a]

[a] State Key Lab of Automotive Energy and Safety, Tsinghua University, Beijing, 100084, People's Republic of China

Version of record first published: 14 Aug 2012.

To cite this article: Shengbo Eben Li , Keqiang Li & Jianqiang Wang (2013): Economy-oriented vehicle adaptive cruise control with coordinating multiple objectives function, Vehicle System Dynamics: International Journal of Vehicle Mechanics and Mobility, 51:1, 1-17

To link to this article: http://dx.doi.org/10.1080/00423114.2012.708421

Vehicle System Dynamics
Vol. 51, No. 1, January 2013, 1–17

Taylor & Francis
Taylor & Francis Group

Economy-oriented vehicle adaptive cruise control with coordinating multiple objectives function

Shengbo Eben Li, Keqiang Li* and Jianqiang Wang

State Key Lab of Automotive Energy and Safety, Tsinghua University, Beijing 100084, People's Republic of China

(*Received 7 June 2011; final version received 28 June 2012*)

A recent design issue of adaptive cruise control systems is how to reduce fuel consumption when following a preceding vehicle. High fuel economy is achievable through reducing acceleration level, however, it is also significantly restrained by two other functional demands, track capability and driver desired response. In the framework of multi-objective coordination, this paper develops and experimentally validates an economy-oriented headway control algorithm for a passenger car with internal combustion engine. The control algorithm is synthesised in a hierarchical structure. The upper controller, undertaking a major coordinating task, is designed based on the model predictive control theory. Fuel economy, tracking capability, and the driver desired response are formulated as its cost function and constraints in a finite prediction horizon. As further analysis indicated, such a design inevitably results in infeasible control inputs in some extreme cases, e.g. urgent situations involving rapid acceleration/deceleration. A constraint softening method is adopted to enlarge the feasible region in the cost of somewhat sacrificing the optimality of the original cost function. Finally, a prototyping controller is developed based on xPC toolbox and equipped in a passenger car. The followed field tests show that, compared to a linear quadratic controller, such an algorithm improves both fuel economy and tracking capability while also being more responsive to driver car-following behaviours.

Keywords: adaptive cruise control; model predictive control; fuel economy; tracking capability

1. Introduction

In an adaptive cruise control (ACC) system, the headway control mode mainly focuses on tracking a target vehicle according to a given headway policy. This task is critical to ACC's function of assisting drivers, e.g. reducing driver workload, because it releases foot manipulation of drivers. Just as drivers with different styles consume different amounts of fuel; the same is true for vehicles with different headway control algorithms [1]. Ioannou has observed a fuel difference of 6% for some commonly-used algorithms in a rapid accelerating scenario [2]. Today, with increasing economy demands in the road transportation sector, this fuel-saving potential is drawing growing attention from automobile manufacturers and government agencies. The

*Corresponding author. Email: likq@tsinghua.edu.cn

ISSN 0042-3114 print/ISSN 1744-5159 online

http://dx.doi.org/10.1080/00423114.2012.708421
http://www.tandfonline.com

related economy-oriented headway control is promising considering large penetration of the ACC into markets in the near future.

Two pioneering studies on this technology, to the best of our knowledge, date back to the beginning of this century. In 2001, Marsden pointed out the feasibility of saving fuel based on his observation that the ACC reduced the standard derivation of acceleration by 44–52% in normal traffic flow [3]. Following Marsden's study, Bose further demonstrated by simulations that this acceleration attenuation decreased about 8% total fuel of a mixed traffic flow [4]. Subsequently, researchers intentionally focus on the algorithm design for the headway control mode in order to decrease fuel consumption to the maximum extent. Today three main strategies have been used in designing: (I) Coordinating control of engine and transmission [5,6]; (II) shorten inter-vehicle distance [7,8]; (III) smooth longitudinal acceleration [2,9,10].

The first strategy regulates engine and transmission simultaneously and aims to increase the probability of engines working in the economic region [5,6]. In the second strategy, shorter inter-vehicle distance means less aerodynamic drag, which in turn reduces external resistances of following vehicles [8]. These two strategies are useful in theory, but their application is significantly limited by high coordinating complexity in Strategy I and additional risks of rear-end collision in Strategy II. In comparison, the last strategy is more realistic under today's technical status. Its basic idea, originating from Marsden's founding, is to reduce the acceleration level as much as possible. Using this strategy, Ioannou *et al.* developed a nonlinear filter for headway controllers to avoid large acceleration in urgent situations [2]. Jonsson *et al.* designed a Dynamic Programming-based off-line controller to depress longitudinal acceleration, with which simulations showed a fuel reduction of 5% [9].

However, reducing acceleration alone is not sufficient in designing an economy-oriented headway control algorithm. Even though a lower level of acceleration in itself implies better economy, it also weakens the tracking capability and enlarges the inter-vehicle distance errors. In an accelerating case, an excessively large distance often induces frequent vehicle cut-ins from adjacent lanes and, in fact, deteriorates fuel economy instead of improving; in a braking case, the excessively short distance may increase the risk of rear-end collision and cause driver's intervention. The most extreme situation, where fuel economy is the exclusive objective, is to always run the vehicle at economic speed, in which case economy becomes optimal while tracking capability is totally lost. Moreover, it is critical to realise that drivers' or passengers' evaluations are an essential component of any ACC efficacy; no matter how effective an ACC model theoretically is, it will be useless if drivers choose not to use it. Therefore, if fuel economy is exclusively emphasised, ACC would scarcely satisfy driver's expectation. This failure may cause drivers to intervene by intermittent foot braking. In such situations, the ACC function of following a predecessor is inevitably lost, let alone assisting drivers, quite apart from its original intention. In summary, when designing an economy-oriented headway control algorithm, it is critical to systematically consider multiple objectives instead of focusing on only one.

In this paper, we first develop and then experimentally verify an economy-oriented headway control algorithm that is designed to optimally coordinate multiple objectives. Here such objectives as high fuel economy, necessary tracking capability and good driver desired response are balanced under the model predictive control (MPC) framework. Better fuel economy remains our first priority, yet great emphasis is also given to necessary tracking capability and good driver desired response. The remainder of this paper is structured as follows. Section 2 reviews the model for the car-following system for control, followed by the quantification of multiple objectives in a finite prediction horizon. Section 3 addresses the issue of the infeasible solution by employing a constraint softening method and achieves its real-time implementation. In Section 4, field tests are conducted to validate this method's success.

2. Synthesis of multi-objective coordinating algorithm

A typical car-following system contains two vehicles, a preceding one and a following one. As in many applications [11,12], its control algorithm is designed using a hierarchical structure composed of a lower and an upper controller. The former compensates for the nonlinear dynamics in vehicle dynamics while the latter conducts the space tracking. The upper controller is synthesised using the MPC framework in this paper, which dominates the coordination of multiple objectives.

2.1. *Car-following model for control*

The following vehicle to be modelled is a passenger car with a 2.0 l gasoline engine, five-speed automatic transmission and hydraulic braking system. Its vehicle longitudinal dynamics are inherently nonlinear. Some salient features include static nonlinearity in engine, discontinuous gear ratio, and quadratic aerodynamic drag [12]. In the lower controller, those nonlinearities are compensated for by using an inverse dynamic model [11]. In addition, a hysteresis switching logic is adopted to avoid the simultaneous actions of driving and braking [13]. The connection of the lower controller and vehicle longitudinal dynamics constructs a virtual plant, whose dynamics is approximated to be linear, as suggested in [10]. Using sinusoidal excitation [14], the connected plant is modelled as a first-order inertial transfer function:

$$a_{\mathrm{f}} = \frac{K_{\mathrm{L}}}{T_{\mathrm{L}}s + 1} a_{\mathrm{fdes}}, \tag{1}$$

where a_{fdes} is the desired longitudinal acceleration, a_{f} is the actual longitudinal acceleration, $T_{\mathrm{L}} = 0.45\,\mathrm{s}$ and $K_{\mathrm{L}} = 1.0$ are time constant and system gain for nominal plants, respectively. By integrating a quadratic headway policy [15] ($d_{\mathrm{des}} = r \cdot (v - v_{\mathrm{fmean}}) + \tau_{\mathrm{h}} \cdot v + d_0$), the dynamic of the car-following system is governed by

$$\begin{bmatrix} \Delta\dot{d} \\ \Delta\dot{v} \\ \dot{a}_{\mathrm{f}} \end{bmatrix} = \begin{bmatrix} 0 & 1 & -\tau_{\mathrm{h}} - r(2v_{\mathrm{f}} - v_{\mathrm{fmean}}) \\ 0 & 0 & -1 \\ 0 & 0 & -1/T_{\mathrm{L}} \end{bmatrix} \begin{bmatrix} \Delta d \\ \Delta v \\ a_{\mathrm{f}} \end{bmatrix} + \begin{bmatrix} 0 \\ 0 \\ K_{\mathrm{L}}/T_{\mathrm{L}} \end{bmatrix} a_{\mathrm{fdes}} + \begin{bmatrix} 0 \\ 1 \\ 0 \end{bmatrix} a_{\mathrm{p}}, \tag{2}$$

where $[\Delta d, \Delta v, a_{\mathrm{f}}]^{\mathrm{T}}$ is the system state denoting distance error, relative speed, and longitudinal acceleration, respectively; a_{fdes} is the control input; a_{p} is the measurable disturbance denoting the preceding vehicle acceleration; v_{f} is the vehicle speed; and τ_{h}, r and v_{fmean} are the parameters of headway policy denoting the headway time, quadratic coefficient, and average speed in experiments, respectively.

Note that Equation (2) has a quasi-linear structure, even though it is still inherently nonlinear because of its speed-dependent coefficients. The nonlinearity helps to enhance the accuracy of predicting system dynamics while also significantly increasing the computing burden of the corresponding MPC controller. Our solution to facilitate computation is to linearise Equation (2) at each sampling point, and to change linearised coefficients as time goes by in order to reflect the speed-varying nonlinearity. The details will be discussed in Section 3.1.

2.2. *Performance index for upper controller*

As suggested by Bageshwar *et al.* [16], an ACC controller with multiple objectives is naturally cast into an MPC framework. Today, MPC has shown great merits in vehicle automation, e.g. [17–19]. Many of them focus on the stability and robustness of cruise control or spacing

tracking. To further expand their application, we introduce multiple objectives in the headway control mode. To design such a controller, one of the key points lies in how to mathematically quantify multiple objectives.

Fuel economy, tracking capability, and driver desired response, including limitations from vehicle dynamics and traffic flow, are interrelated and mutually influenced; each of them shapes ACC behaviours and ACC design should take all of them into account. For simplification, we first discuss their description and then integrate their mathematical formulae into the performance index of MPC. For tracking capability, it is defined as follows:

(A1) The tracking errors converge to zero in the steady-state;
(A2) In accelerating cases, the inter-vehicle states should be in the driver permissible tracking range to avoid frequent cut-ins from adjacent lanes;
(A3) In braking cases, rear-end collision must be avoided whenever physically possible.

With respect to fuel economy, we expect lower fuel consumption than other ACC controllers, denoted as (B). To meet the objective of the driver desired response, ACC should satisfy three vital driver characteristics:

(C1) Driver desired distance feature;
(C2) Driver longitudinal ride comfort;
(C3) Driver car-following (DCF) characteristics.

These three objectives are categorised into two groups and described by a quadratic cost function and three inequality constraints, respectively. Note that (C1), in the form of headway policy, is implicitely embedded into Equation (2) and does not emerge in the performance index. The cost function, which includes (A1), (B) and (C3), is expressed as

$$\begin{aligned} J &= \int_{k\cdot T_\mathrm{s}}^{(k+P)\cdot T_\mathrm{s}} L(\Delta d, \Delta v, a_\mathrm{f}, a_\mathrm{fdes})\,\mathrm{d}t \\ L &= w_{y\Delta d}\cdot\|\Delta d\|^2 + w_{y\Delta v}\cdot\|\Delta v\|^2 \\ &\quad + w_\mathrm{u}\cdot\|a_\mathrm{fdes}\|^2 + w_\mathrm{du}\cdot\|\dot{a}_\mathrm{fdes}\|^2 \\ &\quad + w_{ya}\cdot\|a_\mathrm{fR} - a_\mathrm{f}\|^2, \end{aligned} \tag{3}$$

where T_s is the sampling time, $k\cdot T_\mathrm{s}$ is the current time, $P\cdot T_\mathrm{s}$ is the prediction length, $\|\cdot\|$ represents two-norms, and a_fR is the reference acceleration. In Equation (3), the tracking capability (A1) is specified by penalising both Δd and Δv. Their quadratic integrand operates differently, depending on the quantity of tracking errors, and tends to penalise larger errors and neglect smaller ones. Its minimisation obviously yields that $\Delta d = 0$ and $\Delta v = 0$. The fuel economy (B) is described by minimising a_fdes, as well as its jerk. This minimisation will both smooth and depress the acceleration and accordingly yield better fuel economy. The last term is relevant to the DCF characteristics (C3). When following a speed-changing car, drivers manipulate vehicles according to their own preferences. The preferred acceleration reflects driver desired car-following dynamics [20]. Often, ACCs work in light and moderate congested traffic, and drivers exhibit approximately linear behaviours to the variation of tracking errors. Here, a quasi-linear DCF model is used to imitate driver external manipulating behaviours in car-following scenarios [21]:

$$a_\mathrm{fR} = \mathrm{SVE}(v_\mathrm{f})\cdot k_\mathrm{V}\cdot\Delta v + \mathrm{SDE}(v_\mathrm{f})\cdot k_\mathrm{D}\cdot\Delta d, \tag{4}$$

where, a_fR refers to the reference acceleration. Another reason to use a quasi-linear DCF model is to facilitate real-time implementation of following the MPC controller. The error between

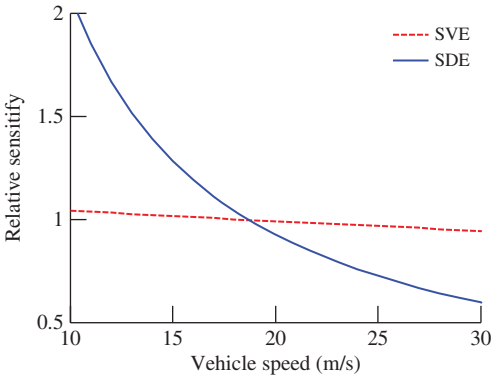

Figure 1. SVE and SDE functions of passenger car drivers.

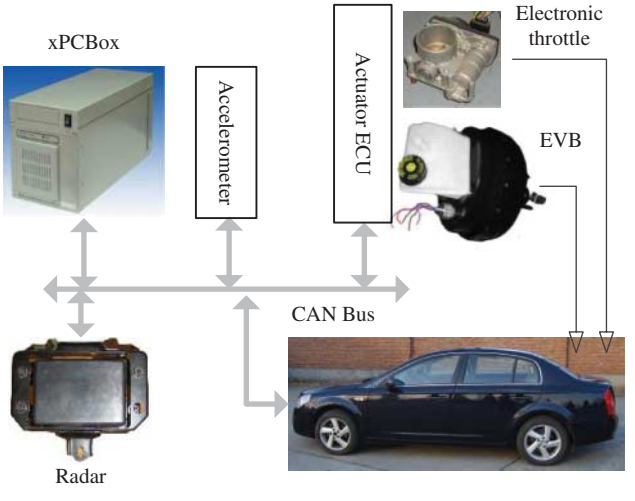

Figure 2. Configuration of experimental platform.

a_{f} and a_{fR} is minimised in order to compel ACC to coincide with the model of DCF dynamics. In Equation (4), k_{V} and k_{D} are nominal control gains, SVE (sensitivity to velocity error) and SDE (sensitivity of distance error) are functions of vehicle speed v_{f}, reflecting the change of control gains w.r.t. vehicle speed v_{f}. Refer to the modelling method introduced in [21], these parameters are identified using experimental data of passenger car drivers in naturalistic traffic flow, yielding $k_{\mathrm{V}} = 0.162$, $k_{\mathrm{D}} = 0.0203$ and SVD/SDE illustrated in Figure 1. (The identified parameters are the average of 33 experienced drivers, including 26 males and 7 females; the traffic scenarios contain urban arterial roads and inter-city expressway.).

Other objectives, including (A2), (A3) and (C3), are more relevant to safety and comfort, suitable to be bounded instead of being optimised:

$$\begin{cases} j_{\mathrm{f\,min}} < j_{\mathrm{fdes}}(t) j_{\mathrm{f\,max}} \\ a_{\mathrm{f\,min}} < a_{\mathrm{fdes}}(t) < a_{\mathrm{f\,max}}, \\ a_{\mathrm{f\,min}} < a_{\mathrm{f}}(t) < a_{\mathrm{f\,max}} \end{cases} \quad t \in [k \cdot T_{\mathrm{s}}, (k+P) \cdot T_{\mathrm{s}}], \tag{5}$$

$$\begin{cases} \Delta \mathrm{d}_{\min} \le \Delta \mathrm{d}(t) \le \Delta \mathrm{d}_{\max} \\ \Delta v_{\min} \le \Delta v(t) \le \Delta v_{\max} \end{cases}, \quad t \in [k \cdot T_{\mathrm{s}}, (k+P) \cdot T_{\mathrm{s}}], \tag{6}$$

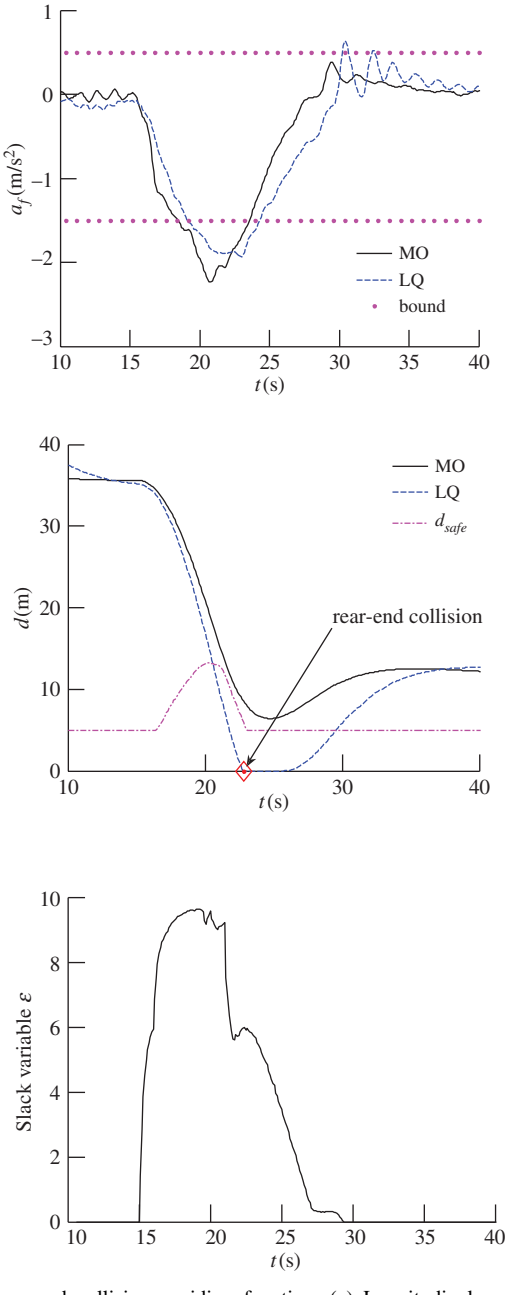

Figure 3. Realisation of rear-end collision avoiding function. (a) Longitudinal acceleration, (b) inter-vehicle distance, and (c) slack variable in MO controller.

$$\begin{matrix} \mathrm{d}(t) \geq d_{\mathrm{safe}} \\ \mathrm{d}_{\mathrm{safe}} = \max\{\mathrm{TTC} \cdot \Delta v, \mathrm{d}_{\mathrm{s0}}\}, \end{matrix} \quad t \in [k \cdot T_{\mathrm{s}}, (k+P) \cdot T_{\mathrm{s}}], \tag{7}$$

where $j_{\mathrm{fmin}}, j_{\mathrm{fmax}}, a_{\mathrm{fmin}}, a_{\mathrm{fmax}}$ are the bounds of jerk and acceleration, d_{safe} is the safety threshold of distance, and Δd_{min}, Δd_{max}, Δv_{min}, and Δv_{max} are the bounds of tracking errors. Note that Δd_{min}, Δd_{max}, Δv_{min}, and Δv_{max} vary with respect to v_{f} to reflect the changes of driver

Table 1. Key parameters in cost function and constraints.

Parameter	Value	Parameter	Value	Parameter	Value
$w_{y\Delta d}$	0.02	$w_{y\Delta v}$	0.025	w_{ay}	0.5
$w_{u\_}$	5	w_{du}	0.001	T_s	0.1 s
$\Delta\bar{d}_{\max}$	7.2 m	$\Delta\bar{v}_{\max}$	0.8 m/s	$a_{f\max}$	0.5 m/s^2
$\Delta\bar{d}_{\min}$	−6.7 m	$\Delta\bar{v}_{\min}$	−0.8 m/s	$a_{f\min}$	−1.5 m/s^2
TTC	−2.5 s	d_{s0}	5 m	P	50

sensitivity:

$$\begin{aligned}\Delta d_{\min} &= SDE(v_f)\cdot\Delta\bar{d}_{\min},\ \Delta d_{\max} = SDE(v_f)\cdot\Delta\bar{d}_{\max}\\ \Delta v_{\min} &= SVE(v_f)\cdot\Delta\bar{v}_{\min},\ \Delta v_{\max} = SVE(v_f)\cdot\Delta\bar{v}_{\max}.\end{aligned} \tag{8}$$

Equation (5) represents ride comfort demand from drivers. This demand constrains both acceleration and jerk, as suggested in [22]. Equation (6) constrains both Δd and Δv to avoid overly large or overly short tracking errors. This constraint originates from the driver permissible tracking range, identified based on naturalistic driver experiments. When tracking errors are bounded in this range, vehicle cut-in or driver intervention does not easily occur and accordingly the tracking process becomes more smoothing, which is also helpful to fuel economy. Safety means no rear-end collisions, always maintaining a nonnegative inter-vehicle clearance. The time-to-collision (TTC) strategy is used to restrain minimum distance [23]. Together with minimum distance strategy, Equation (7) is designed, in which d_{safe} refers to the safety threshold.

2.3. *Analysis of multi-objective coordination*

Under the MPC framework, the control input actually results from solving an optimisation problem originated from a cost function and relevant constraints. We call such an MPC controller as a multi-objective coordinating algorithm, abbreviated as MO. Some key parameters are shown in Table 1.

In MO, particular focus is placed on reducing longitudinal acceleration since our primary goal is high fuel economy. Therefore, relatively large weighting coefficients for a_f and $\underline{a}_{\underline{f}des}$ are selected compared to those for Δd and Δv, as shown in Table 1. The optimisation of J in Equation (3) is approximately equivalent to an exclusive minimisation on acceleration, which is rather beneficial in improving fuel economy. In addition, great benefit is also gained in numerical computation because such a cost function will lead to a quadratic programming (QP) problem rather than a complicated nonlinear programming problem. Nevertheless, the weighting coefficients of Δd and Δv still exist for controller stabilisation. Since stabilisation implies convergence, tracking errors converge in steady scenarios and therefore (A1) naturally holds. The reference acceleration a_{fR} in Equation (3) originates from the DCF model and reflects driver desired acceleration in a car-following process. Therefore, the minimisation of the error between a_f and a_{fR} will compel the ACC to conform to driver's expectation, satisfying (C3).

Inequality (5) restricts a_{fdes} and a_f in order to meet (B2), which not only enhances ride comfort, but also avoid fuel-wasting urgent acceleration/deceleration. As discussed before, fuel improvement will decrease tracking capability in an ACC. In MO, severe drop in tracking capability is limited by strict constraints on tracking errors, as shown in Equation (6). Its goal is to constrain excessively large tracking errors and avoid frequent vehicle cut-ins or driver

intervention. Additionally, Inequality (7) stipulates the permissible minimum distance and accordingly any rear end collision will be avoided whenever physically possible.

3. Real-time algorithm with feasible solutions

In MPC, Equation (5)–(7) are referred to as hard constraints because their bounds were not allowed to be violated. Meanwhile Equation (5) weakens the accelerating/decelerating ability and tracking errors sometimes unavoidably reach their bounds. To avoid overshooting tracking errors, a reasonable approach is to strengthen the control input. However, in practice, this is unrealistic because the control input is almost always located on its upper bound in accelerating scenarios, leaving no space to be increased further. A similar conclusion is also obtained in braking scenarios. At this moment, the tracking errors keep increasing or decreasing along their original directions due to vehicle inertia. Once overshooting occurs, the optimisation problem has no feasible solution, resulting in the issue of infeasibility.

3.1. *Constraint softening method*

One effective way to address infeasibility is called the constraint softening method [24]. Its fundamental is to transform hard constraints into soft constraints by enlarging the bounds whenever states or inputs overshoot. There are two common types of constraint softening methods according to their slack variables: vector variables and scale variables [25,26]. The former independently softens each inequality in constraints, but considerably increases the dimension of optimised variables, thus affecting the computing efficiency of the optimisation problem. The latter regards all the inequalities as an integral, adds only one new optimised variable, and has little effect on efficiency. We adopted a scalar slack variable to soften the hard constraints considering the demand of real-time implementation.

A new cost function with a slack variable ε is defined:

$$\psi = J + \rho\varepsilon^2, \quad \varepsilon \geq 0, \tag{9}$$

where ρ is the weighting coefficient. The constraints (5) and (6) are transformed into soft constraints in $[k \cdot T_s, (k+P) \cdot T_s]$:

$$a_{\min} + \varepsilon \cdot v_{\min}^{a_f} \leq a_{f\mathrm{des}}(k|i) \leq a_{\max} + \varepsilon \cdot v_{\max}^{a_f}, \tag{10}$$

$$\begin{cases} \Delta \mathrm{d}_{\min} + \varepsilon \cdot v_{\min}^{\Delta d} \leq \Delta \mathrm{d}(k|i) \leq \Delta \mathrm{d}_{\max} + \varepsilon \cdot v_{\max}^{\Delta d} \\ \Delta v_{\min} + \varepsilon \cdot v_{\min}^{\Delta v} \leq \Delta v(k|i) \leq \Delta v_{\max} + \varepsilon \cdot v_{\max}^{\Delta v}, \\ a_{\mathrm{f}\,\min} + \varepsilon \cdot v_{\min}^{a_f} \leq a_{\mathrm{f}}(k|i) \leq a_{\mathrm{f}\,\max} + \varepsilon \cdot v_{\max}^{a_f} \end{cases} \tag{11}$$

where $v_{\min}^{\#}$ and $v_{\max}^{\#}$ are relaxation coefficients. The superscript # stands for Δd, Δv or a_f. Here, Equations (10) and (11) are called soft constraints because their bounds are allowed to be violated. Thereafter, the coordinated control of multiple objectives is realised by solving the following optimisation problem (12):

$$\begin{aligned} &\min_{a_{f\mathrm{des}}(t)} \quad \psi(k), t \in [k \cdot T_s, (k+P) \cdot T_s] \\ &\text{Subject to:} \quad \text{(a) Plant model} - \text{Equation (2);} \\ &\qquad\qquad\quad \text{(b) Soft constraints} - \text{Equations (10) and (11);} \\ &\qquad\qquad\quad \text{(c) Hard constraints} - \text{Equation (7).} \end{aligned} \tag{12}$$

In Problem (12), when hard constraints (5) and (6) do not hold, the slack variable ε automatically becomes positive. Even the constrained variables, e.g. Δv and Δd, violate their bounds, Equations (10) and (11) will still hold because of their ε-dependent bounds. The violation, however, is not completely free, limited by penalising ε in the cost function (9), and therefore a balance between constraint violation and control optimality is sought. When original constraints (5) and (6) hold, the slack variable ε becomes zero and Problem (12) is equivalent to the problem with hard constraints.

Here the constraint (7) is not allowed to be violated for safety considerations. Moreover, to retain it, as hard constraint does not cause any issue of infeasibility because of the following reasons. In Problem (12), all constraints are defined in the prediction horizon $[k \cdot T_s, (k+P) \cdot T_s]$. When the preceding vehicle decelerates rapidly in an urgent situation, d at time $(k+P) \cdot T_s$ always reaches the safety threshold d_{safe} in advance of d at time $(k \cdot T_s)$ due to prediction. In such a case, Problem (12) always decreases a_{fdes} at time $(k+P) \cdot T_s$ to avoid the violation of $d((k+P) \cdot T_s)$. Since the constraint on a_{fdes} is softened in the whole prediction horizon, this will increase ε and strengthen the braking force at time $k \cdot T_s$. Consequently, the risk of rear-end collision is still capable of being eliminated without causing any infeasibility.

3.2. *Numerical computation*

Considering MPC is usually implemented in a discrete-time domain, we need to transform the time-continuous Problem (12) into a time-discrete form (15) at a specified sampling time T_s.

Note that Equation (2) is quasi-linear and its coefficients are time-varying, dependent on vehicle speed. In theory, its discretisation is relatively difficult because an analytical solution of integration of nonlinear matrix does not exist. To avoid this issue, we combine the piece-wise linearisation [27] and T–S (Takagi–Sugono) fuzzy modelling technology [28], and construct a discrete-time state space model with a unique formula. The procedure of discretisation is: (1) firstly, select two speed points $v_{fHigh} = 25\,\mathrm{m/s}$ and $v_{fLow} = 10\,\mathrm{m/s}$ to represent highway and city road traffic flow, respectively; (2) then, discretise equation (1) at each speed using the zero-order hold method, yielding two linear models; (3) finally, the two models are weighted and summed, thereby obtaining a piece-wise state space model:

$$\begin{aligned}
\begin{bmatrix} \Delta \mathrm{d}(k+1) \\ \Delta v(k+1) \\ a_f(k+1) \end{bmatrix} &= A(\lambda) \begin{bmatrix} \Delta d(k) \\ \Delta v(k) \\ a_f(k) \end{bmatrix} + B(\lambda) a_{fdes}(k) + G(\lambda) a_p(k) \\
A(\lambda) &= \lambda A_{High} + (1-\lambda) A_{Low} \\
B(\lambda) &= \lambda B_{High} + (1-\lambda) B_{Low} \\
G(\lambda) &= \lambda G_{High} + (1-\lambda) G_{Low},
\end{aligned} \tag{13}$$

where $A_{\#}$, $B_{\#}$ and $G_{\#}$ are system matrices of discrete-time models and the subscript # is 'High' or 'Low', representing v_{fHigh} or v_{fLow}; λ is so-called T–S factor, defined as function of speed:

$$\lambda = \begin{cases} 0 & v_f < v_{fLow} \\ (v_f - v_{fLow})\,(v_{fHigh} - v_{fLow})^{-1}, & v_{fLow} \le v_f \le v_{fHigh} \\ 1 & v_f > v_{fHigh} \end{cases}. \tag{14}$$

Here, Equation (13) is still inherently nonlinear because of its speed-varying system matrices via the T–S factor λ. Nevertheless, the computing efficiency is considerably enhanced. In different sampling times, λ varies with vehicle speed for accurate prediction of plant dynamics. During each sampling period, λ is assumed to be fixed and the MPC algorithm becomes

linear, capable of being more efficiently computed. Moreover, the change of vehicle speed is always small because the prediction horizon is short ($P = 50$ and $P \cdot T_s = 5$ s). Therefore, the assumption that λ is fixed in each sampling period is reasonable. The same discretising strategy is applied to cost function and constraints. A detailed discussion of discretisation is beyond the scope of this paper, but can be found in Maciejowski's book [25]. Now, rewriting the MPC controller in the discrete-time domain, we have:

$$
\begin{aligned}
&[j^*_{\text{fdes}}(k+i|k)|_{i=0:P-1}, \varepsilon^*(k)] = \arg \min_{j_{\text{fdes}}(k+i|k)|_{i=0:P-1}, \varepsilon(k)} \psi(k,i), \quad i = 1:P,\\
&\text{Subj. to :}\\
&\quad \text{(a) Time-discrete form of model (2), that is Equation (13)}\\
&\quad \text{(b) Time-discrete form of constraints (10), (11);}\\
&\quad \text{(c) Time-discrete form of constraint (7);}
\end{aligned}
\tag{15}
$$

Where $j_{\text{fdes}}(k)$ is the desired longitudinal jerk, $(k+i|k)$ denotes the predicted value at the $(k+i)$th step based on kth step information.

The last stage of real-time implementation is to numerically optimise Problem (15) in the specified time T_s. Because Problem (15) naturally leads to a QP, a Dantzig–Wolfe active set algorithm [29] is selected to compute the optimal desired jerk $[j_{\text{fdes}} * (k+i|k)]_{i=1:P}$ and the optimal slack variable $\varepsilon * (k)$. In each sampling time, only the head element $j_{\text{fdes}} * (k+0|k)$ is adopted to compute the optimal control input:

$$
a_{\text{fdes}}(k) = a_{\text{fdes}}(k-1) + j^*_{\text{fdes}}(k+0|k) \cdot T_s, \tag{16}
$$

where $a_{\text{fdes}}(k-1)$ is the control input in the last step.

4. Performance verification

4.1. *Experimental platform*

The experimental platform is constructed based on a sedan with a 2.0 l gasoline engine and a five-speed automatic transmission. The configuration is shown in Figure 2. The radar detects the target car ahead and calculates the inter-vehicle states, including both Δd and Δv. The three-axis accelerometer measures longitudinal, lateral and vertical acceleration. The preceding vehicle's acceleration is estimated via both radar outputs and acceleration measurements. This information, together with vehicle states, are sent to the xPC© box via a data-sharing CAN bus. In the xPC box, the Dantzig–Wolfe algorithm is programmed using C++; other functional modules, e.g. the lower controller, switch logic, radar signal processing, actuator controllers and human machine interface, are built with Matlab/Simulink©. The actuator ECU regulates the electronic throttle and EVB (Electronic Vacuum Booster) to track the desired commands.

A standard linear quadratic regulator (simply notated by LQ) is designed referring to [11] as a comparison. No external disturbance is assumed to exist in this LQ regulator (external disturbance is the preceding vehicle's acceleration). Moreover, its cost function, including coefficients, is identical to MO, except that it has no terms of acceleration error and longitudinal jerk. In LQ, a linear model is necessary, and it is derived from Equation (13) by fixing v_p at 15 m/s. In addition, there is no constraint in LQ.

In experiments, a 'virtual' preceding vehicle is used, instead of a real leading car. 'Virtual' means that the radar outputs are imitated in software, including the imperfection of radar and

data processing, e.g. signal noise in MMW reflection, digital quantisation and limited update rate in CAN bus, etc. The purpose of using a virtual leading car is (1) to avoid unpredictable danger in case of system malfunction; (2) to provide repeatable and identical speed profiles for controller comparison. The experiment scenarios are designed based on commonly existing traffic flow, including: (a) a rapid braking scenario; (b) sinusoidal speed scenario; (c) highway and city road driving cycles used in ISUZU Ltd. The MO is considered to be successful if it improves fuel economy while not sacrificing tracking capability and the driver desired response.

4.2. *Rapid braking scenario*

In this scenario, the preceding car rapidly decelerates from 15 m/s to 1 m/s at a deceleration of $-2.5\,\mathrm{m/s^2}$. The ACC car follows it at the same initial speed of 15 m/s with the initial distance error of zero.

In this scenario, the inter-vehicle distance quickly decreases because the preceding vehicle brakes rapidly. Figure 3(a) shows that LQ provides insufficient deceleration due to relatively small coefficients of tracking errors in its cost function. At 23 s, the distance becomes zero and a rear-end collision occurs. In contrast, as shown in Figure 3, MO automatically increases both the slack variable ε and the braking force when distance approaches the safety threshold, and thereby effectively eliminates the risk of a rear-end collision caused by the pursuit of high fuel economy.

4.3. *Sinusoid speed scenario*

The experiment in this scenario lasts for 60 s. The preceding car runs at a sinusoid speed profile with initial speed 10 m/s and acceleration amplitude $0.6\,\mathrm{m/s^2}$. The ACC car has an initial speed of 8 m/s. Figure 4 shows the experimental results of the first 50 s, and Figure 5 shows the phase plots of $v_\mathrm{f} - \Delta d$ in two time sections, 0–25 s and 37–57 s. In these figures, the pink dotted line represents the original bound and the red dot-dash line represents the reference trajectory dominated by the DCF model.

Because of the nonzero initial Δv, the whole experiment results contained two stages: a transient stage from 0 to 20 s and a steady stage from 20 s to the end.

In the transient stage, due to the large initial state error, both LQ and MO tend to adopt large acceleration for faster state convergence. The MO constrains its desired acceleration while the LQ does not as shown in Figure 4(a). This constraint on acceleration not only helps improve ride comfort, but also decreases engine fuel rate, as shown in Figure 4(e). Neverthless, both MO and LQ output state trajectories that considerably deviate from the reference. After entering the steady-stage, however, the acceleration constraint in MO becomes inactive. As Figure 5(b) shows, the MO trajectory is much closer to the reference than LQ. This indicates that the minimisation of the error between a_f and a_fR in MO has gone into effect, and its car-following dynamics better agrees with passenger driver's expectation (which is imitated by the DCF model).

Table 2 summarises the fuel consumption in experiments. While it is apparent that MO improves fuel economy compared to LQ, this improvement is at the cost of enlarging tracking errors. As shown in Figure 4(c), MO outputs a distance larger than LQ, especially in the transient stage, but this enlargement does not obviously sacrifice the tracking capability because the distance error is still within the driver permissible tracking range.

In addition, even though the tracking errors may exceed their permissible tracking range in some urgent scenarios, MO increases the slack variable and intensifies acceleration or deceleration to reduce excessive tracking errors. This behaviour has been explicitly demonstrated

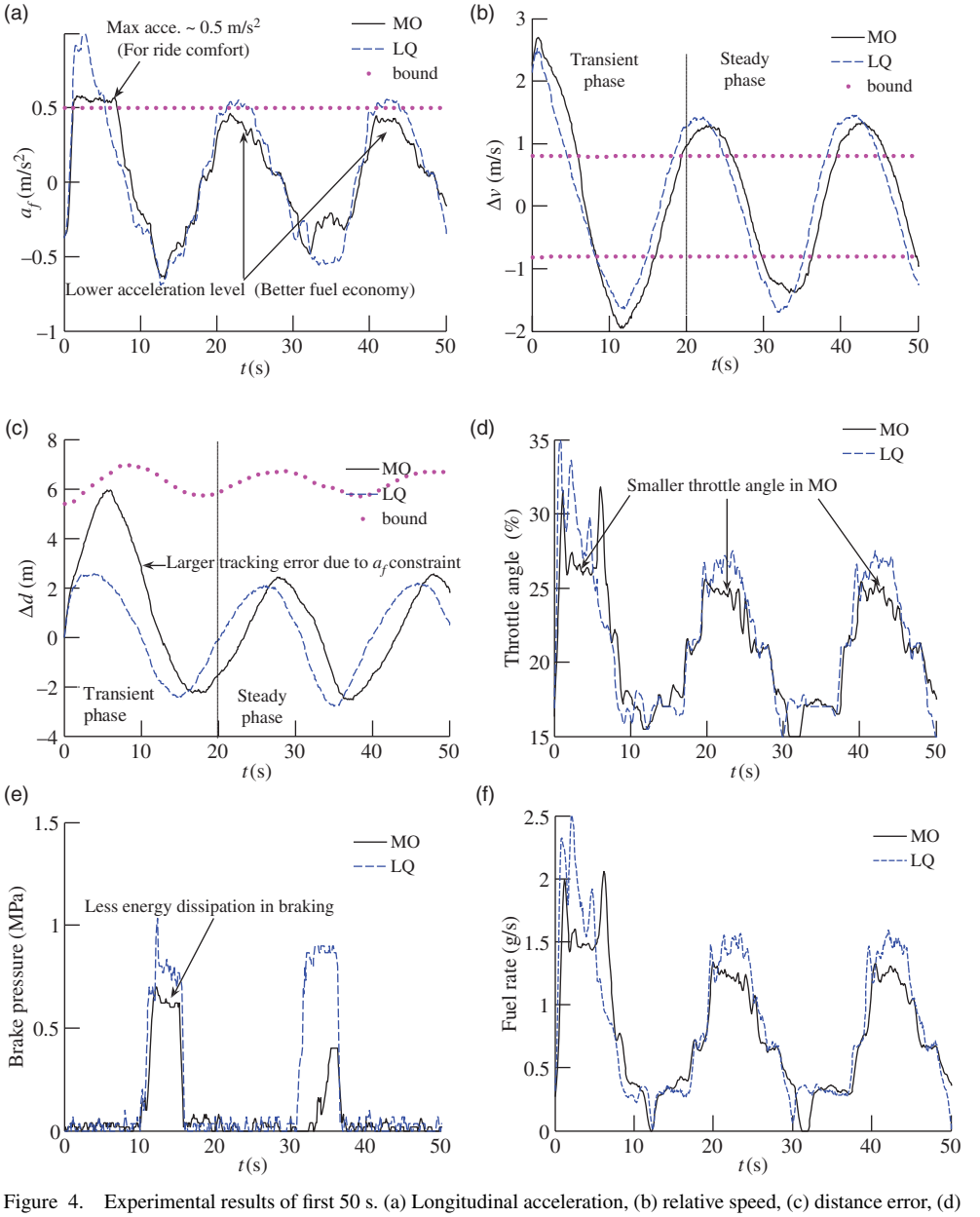

Figure 4. Experimental results of first 50 s. (a) Longitudinal acceleration, (b) relative speed, (c) distance error, (d) throttle angle of engine, (e) braking pressure of braking system and (f) fuel rate of engine.

in Section 4.2. Even in the sinusoidal speed scenario, we can also see similar outputs in MO. For instance, the slack variable ε increases whenever Δv overshoots its bounds as illustrated in Figure 4(b). It implies that stronger suppression must be implemented on Δv. That is, for the reason that the maximum of Δv in MO is smaller than LQ in the steady stage.

4.4. *City road and highway driving cycles*

In order to verify the performance comprehensively, two driving cycles are adopted to represent typical city road and highway traffic flow (Profiles come from IZUZU Ltd.). Their speed

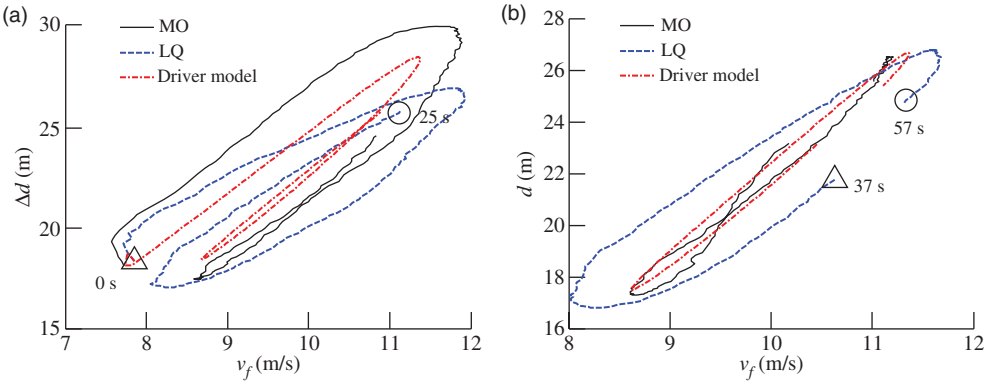

Figure 5. Comparison of driver and ACC car-following dynamics. (a) Phase plot of $v_f - \Delta d$ in transient stage (0–25 s) and (b) phase plot of $v_f - \Delta d$ in steady stage (37–57 s).

Table 2. Total fuel consumption in the experiment.

	LQ	MO	Save
Fuel consumption	50.9	47.1	8.1%

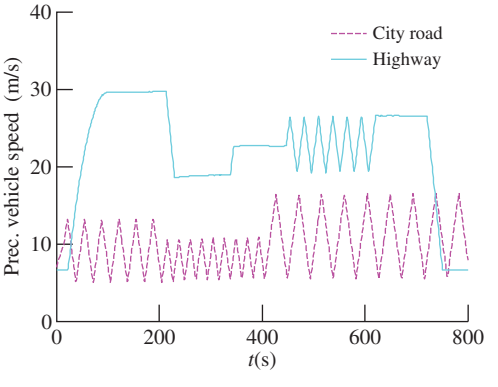

Figure 6. City road and Highway driving cycles.

profiles are illustrated in Figure 6. Similar to Sections 4.1 and 4.2, the ACC car is controlled to follow the 'virtual' preceding vehicle by the MO and LQ, respectively.

To comprehensively reflect tracking capability, define a tracking index (TI) composed of both Δv and Δd as

$$\mathrm{TI} = \frac{1}{N}\sum_{i=1}^{N}\left(|\Delta v(i)\cdot \mathrm{SVE}| + \left|\frac{\Delta d(i)\cdot \mathrm{SDE}}{K_{\mathrm{DV}}}\right|\right), \tag{17}$$

where N is the length of driving cycle, K_{DV} is the weighting coefficient, reflecting different emphasis on Δd and Δv. Here, K_{DV} is selected as 10 for passenger drivers. The TI value under city road and high way driving cycles is shown in Figure 7. The corresponding fuel index (FI), in unit litre per 100 km (l/100 km), is shown in Figure 8. Additional experimental results are summarised in Tables 3 and 4.

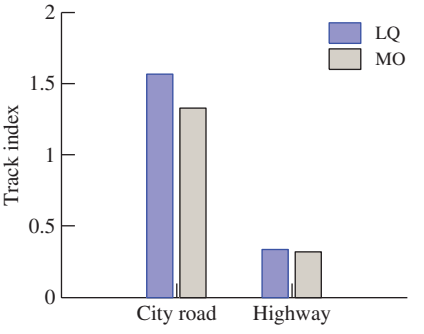

Figure 7. Comparison of tracking capability.

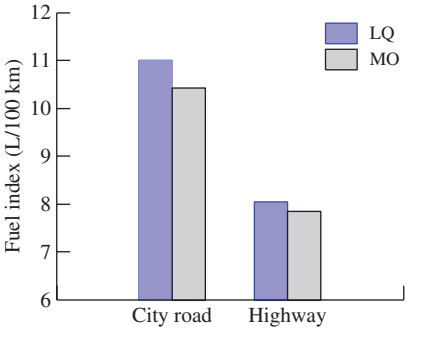

Figure 8. Comparison of fuel economy.

Table 3. City road driving cycle.

	Units	MO	LQ	Improvement
Fuel cons.	Litre	0.77	0.81	–
Mileage	km	7.4	7.4	–
FI	l/100 km	10.4	11.0	5.3%
Tracking index	–	1.33	1.56	14.9%

Table 4. Highway driving cycle.

	Units	MO	LQ	Improvement
Fuel cons.	Litre	0.81	0.83	–
Mileage	km	10.3	10.3	–
FI	l/100 km	7.8	8.1	2.5%
Tracking index	–	0.31	0.33	1.8%

In the city road driving cycle, MO reduces the FI by 5.3% compared to LQ, and the tracking index is reduced by 14.9%. The highway driving cycle involves less aggressive driving, and therefore both fuel economy and tracking capability are only slightly improved, with improvement of 2.5% and 1.8%, respectively.

The city driving cycle better demonstrates the success of imitating DCF characteristics due to richer accelerating and decelerating scenarios. Figure 9 shows that MO outputs a trajectory closer to the reference than LQ because of the introduction of a DCF model in the controller

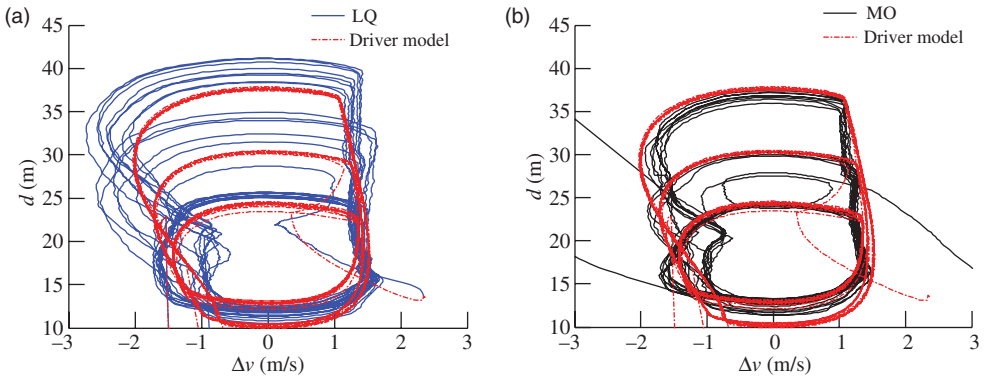

Figure 9. Comparison of driver desired response. (a) LQ algorithm and (b) MO algorithm.

design. This imitation to the DCF model has the potential to improve driver desired response, thus making an ACC more acceptable as an assistant system.

4.5. *Complementary explanation*

Both MO and LQ belong to optimal controllers, but their outputs are of significant difference despite their similar cost function. Experiment results demonstrate that MO decreases fuel consumption further while not sacrificing, or even improves, tracking capability and the driver-desired response. This improvement on multiple objectives can be ascribed to two intrinsic differences of the two controllers:

(1) The implementation of LQ has an implicit assumption, no external disturbance. A car-following system actually has external disturbances in the form of the preceding vehicle's acceleration, which makes a standard LQ regulator somewhat lose its optimality. In comparison, MO can predict the external disturbance and take advantage of this prediction, thereby achieving better comprehensive performances than a standard LQ regulator.
(2) Nonlinearity and constraint in plants are another reason for two controllers' difference in performance. In theory, MPC is capable of optimally controlling constrained nonlinear plants in each step while LQ cannot. Since the plant in this paper is nonlinear and constrained, it is not surprising that LQ is somewhat worse in performance than MPC.

5. Conclusions

We developed and experimentally verified in this paper an economy-oriented headway control algorithm for ACC, which possessed a function of simultaneously dealing with multiple objectives: high fuel economy, necessary tracking capability and a good driver desired response. It is concluded that:

(1) For internal combustion engine vehicles, reducing longitudinal acceleration level is an effective way to improve fuel economy. However, reducing acceleration alone is not a sufficient exclusive objective in designing an economy-oriented headway control algorithm. The requirements from automation and drivers also significantly shape the behaviours of ACC, and consequently affect the improvement of fuel consumption.

(2) The introduction of a driver permissible tracking range helps to avoid cut-ins from adjacent lanes. The integration of a DCF model coincide ACC with DCF characteristics, and it has the potential to avoid unnecessary driver intervention caused by a driver's feelings of discomfort.
(3) The MPC framework is capable of dealing with multiple interactive objectives in a economy-oriented ACC. The field test results demonstrate that the designed MO algorithm can reduce both fuel consumption and tracking errors of the ACC vehicle while not sacrificing driver desired response.

Acknowledgements

The research work was partially supported by NSF China with 51205228 and National 863 Plan of China with 2011AA110402. The authors highly appreciate Mr Hiroshi Ukawa and Mr Dongsheng Bai in ISUZU for their continuous support on design, coding and tests. Many enlightening discussion with Prof. Rajesh Rajamani in University of Minnesota is also gratefully acknowledged.

References

[1] S. Tsugawa, *An overview on energy conservation in automobile traffic and transportation with ITS*, Proc. of IEEE Intl. Veh. Electron. conf., Tottori, Japan, 2001, pp. 137–142.
[2] J. Zhang and P. Ioannou, *Longitudinal control of heavy trucks in mixed traffic: Environmental and fuel economy considerations*, IEEE Trans. Intel. Transp. Syst. 7(1) (2006), pp. 92–104.
[3] G. Marsden, M. McDonald, and M. Brackstone, *Towards an understanding of adaptive cruise control*, Trans. Res. C Emerg. Tech. 9(1) (2001), pp. 33–51.
[4] A. Bose and P. Ioannou, *Analysis of traffic flow with mixed manual and semi-automated vehicles*, IEEE Trans. Intell. Transp. Syst. 4(4) (2003), pp. 173–188.
[5] J. Ino, T. Ishizu, and H. Sudou, *Adaptive cruise control system using CVT gear ratio control*, SAE Trans. 110(7) (2001), pp. 675–680.
[6] S. Li, Y. Bin, and K. Li, *A control strategy of ACC system considering fuel consumption*, Proc. of 2006 AVEC conf., Taipei, China, 2006, pp. 851–855.
[7] M. Shida, T. Doi, Y. Nemoto, and K. Tadakuma, *A short-distance vehicle platooning system 2nd report – evaluation of fuel savings by the developed cooperative control*, Proc. of 2010 AVEC conf., Loughborough, UK, 2010.
[8] M. Hammache and M. Michaelian, *Aerodynamic forces on truck models, including two trucks in tandem*, California PATH Research Report, 2001. Available at http://escholarship.org/.
[9] J. Jonsson, *Fuel optimized predictive following in lower speed conditions*, Master thesis, Linköping, Linköping University, 2003.
[10] S. Li, K. Li, J. Wang, L. Zhang, X. Lian, H. Ukawa, and D. Bai, *Model predictive control based adaptive cruise control considering both tracking capability and fuel economy*, IEEE VPPC 2009, Harbin, China, 2009.
[11] K. Yi and Y. Kwon, *Vehicle-to-vehicle distance and speed control using an electronic-vacuum booster*, JSAE Rev. 22 (2004), pp. 403–412.
[12] R. Rajamani, *Vehicle Dynamics and Control*, Springer, New York, 2006.
[13] J. Gerdes and J. Hedrick, *Vehicle speed and spacing control via coordinated throttle and brake actuation*, Control Eng. Pract. 5(11) (1997), pp. 1607–1614.
[14] R. Pintelon and J. Schoukens, *System Identification – A Frequency Domain Approach*, IEEE Press, New York, 2001.
[15] J. Zhou and H. Peng, *Range policy of adaptive cruise control vehicles for improved flow stability and string stability*, IEEE Trans. ITS 6(2) (2005), pp. 229–237.
[16] V. Bageshwar, W. Garrard, and R. Rajamani, *Model predictive control of transitional maneuvers for adaptive cruise control vehicles*, IEEE Trans. Veh. Technol. 53(5) (2004), pp. 365–374.
[17] T. Coen, J. Anthonis, and J. De Baerdemaeker, *Cruise control using model predictive control with constraints*, Comput. Electron. Agric. 63(2) (2008), pp. 227–236.
[18] D. Corona and B. Schutter, *Adaptive cruise control for a smart car: A comparison benchmark for MPC-PWA control methods*, IEEE Trans. Control Syst. Technol. 16(2) (2008), pp. 365–372.
[19] E. Hellström, M. Ivarsson, J. Åslund, and L. Nielsen, *Look-ahead control for heavy trucks to minimize trip time and fuel consumption*, Control Eng. Pract. 17(2) (2009), pp. 245–254.
[20] S. Panwai and H. Dia, *Comparative evaluation of microscopic car-following behavior*, IEEE Trans. ITS 6(3) (2005), pp. 314–325.
[21] S. Li, J. Wang, K. Li, X. Lian, H. Ukawa, and D. Bai, *Modeling of heavy-duty truck driver's car-following characteristics and its verification*, Int. J. Automot. Technol. 11(1) (2010), pp. 81–87.

[22] P. Ioannou and Z. Xu, *Throttle and brake control systems for automatic vehicle following*, IVHS J. 1(4) (1994), pp. 345–377.
[23] J. Lee, D. McGehee, T. Brown, and M. Reyes, *Collision warning timing, driver distraction, and driver response to imminent rear-end collisions in a high-fidelity driving simulator*, Hum. Factors 44(2) (2002), pp. 314–334.
[24] R.K. Mutha, W.R. Cluett, and A. Penlidis, *Nonlinear model-based predictive control of control non affine system*, Automatica 33(5) (1997), pp. 907–913.
[25] J. Maciejowski, *Predictive Control with Constraints*, Pearson Education, London, 2002.
[26] P.O.M. Scokaert and J.B. Rawlings, *Feasibility issues in linear model predictive control*, Proc. Syst. Eng. 45(8) (2004), pp. 1649–1659.
[27] A. Rantzer and M. Johansson, *Piecewise linear quadratic optimal control*, IEEE Trans. Autom. Control 45(4) (2000), pp. 629–637.
[28] C. Tseng, B. Chen, and H. Uang, *Fuzzy tracking control design for nonlinear dynamic systems via T-S fuzzy model*, IEEE Trans. Fuzzy Syst. 9(3) (2001), pp. 381–392.
[29] R. Fletcher, *Practical Methods of Optimization*, John Wiley & Sons, Chichester, 1987.